Lasers in Medical Science (2019) 34:1–10
https://doi.org/10.1007/s10103-018-2567-9

ORIGINAL ARTICLE

Adipose-derived mesenchymal stem cells treatments for fibroblasts of fibrotic scar via downregulating TGF-β1 and Notch-1 expression enhanced by photobiomodulation therapy

Bing Han[1] · Jincai Fan[1] · Liqiang Liu[1] · Jia Tian[1] · Cheng Gan[1] · Zengjie Yang[1] · Hu Jiao[1] · Tiran Zhang[1] · Zheng Liu[1] · Hua Zhang[1]

Received: 8 December 2017 / Accepted: 14 June 2018 / Published online: 26 October 2018

Keywords AMSCs · PBMT · fibrosis · TGF-β1 · Notch-1

Introduction

Wounds of skin often heal with scar formation. Generally, adverse scar (keloid or hypertrophic scar) formation is characterized with negative cosmetic and psychological effects. Various therapeutic approaches have been studied for keloid and hypertrophic scar, which include occlusive dressings, local injection, surgical excision, etc. [1–6]. Some identified genetic, systemic, and local factors make contributions to the pathogenesis of keloid and hypertrophic scar [7–10]. And local mechanical forces also play a significant role in the formation of adverse scar [11, 12]. Previous studies demonstrate that epithelial-mesenchymal transition (EMT) and myofibroblast transition plays an important role in aberrant scar formation, which can be induced by a regulatory network formed by multiple signaling pathways, especially transforming growth factor beta 1 (TGF-β1) as a critical driver [13–16]. Similarly, TGF-β1-induced EMT can also be meditated by other signaling pathways through direct interactions or transcription [17–19]. Notch signaling, an evolutionarily conserved pathway that regulates multiple cellular process, was proved to play a key role in regulating fibroblast activation and EMT [20, 21]. And interestingly, a great body of evidence supports that TGF-β and Notch signaling regulate EMT and fibrogenesis cooperatively [22–24]. However, understanding into the keloid and hypertrophic scar pathogenesis is still lacking, which contributes to less proper treatment strategies. As lately studies show that formation of these abnormal scars share several pathological processes with other fibrotic diseases, and may occur as a result of fibroproliferative disorder [10, 25]. And increasing evidence indicates that mesenchymal stem cells (MSCs) has been a potential treatment for fibroproliferative disorder by recruitment of macrophage and T cell, upregulation of vascular endothelial growth factors and initiation of angiogenesis, secretion of anti-fibrotic factors, promotion of dermal fibroblast functions, and differentiation into cutaneous cell types [26–29].

Among the MSCs, adipose-derived mesenchymal stem cells (ADSCs) with advantages of abundant in source of tissue, easy to harvest, minimal donor site injury, and fine histocompatibility has drawn attention from scientists. Recently, evidence support that use of ADSCs can remodel fibrotic matrix in a scar, as well as reduce the proliferation, extra cellular matrix (ECM) production, and contraction of myofibroblasts. Also, levels of profibrotic factor TGF-β1 decreased while pro-angiogenic factors vascular endothelial growth factor (VEGF) increased [30–33]. Together, we surmise that growth factors and cytokines of AMSC have the potential to prevent or even to reverse fibrosis. Yet the mechanisms of how AMSCs work in treatment of fibrosis have not been thoroughly investigated.

Photobiomodulation therapy (PBMT), used to be known as low level laser treatment (LLLT), or low level light treatment (LLLT) is considered as a laser or light

Electronic supplementary material The online version of this article (https://doi.org/10.1007/s10103-018-2567-9) contains supplementary material, which is available to authorized users.

✉ Jincai Fan
1012980819@qq.com

[1] Ninth Department of Plastic Surgery, Plastic Surgery Hospital of Chinese Academy of Medical Sciences, No. 33, Ba-Da-Chu Road, Beijing, China

with low power and energy, when act on tissues, which can induce positive photobiological processes in cells compared to the same light delivered at high doses [34, 35]. At molecular and cellular level, photons emitted by PBMT devices are absorbed by mitochondria, and then the production of ATP is elevated, yet levels of ROS remains low, which paly a pivotal role in activation of transcription factors, to produce a number of gene transcript products responsible for the positive effects of PBMT [36]. Given that laser biostimulation theory, PBMT was used in many kinds of cells to investigate its influence on cell proliferation and differentiation. Among those cells, AMSCs and other kinds of mesenchymal stem cells have been frequently investigated [37–40]. Studies have shown that PBMT might generate stimulatory benefits of ADSCs, such as regulating cell secretion, promoting cells proliferation, differentiation and migration, enhancing immunological functions, and, therefore accelerating tissue repairing [41–45]. However, the parameters of lasers used in previous studies have varied, and various effects have been observed when differing type, wavelength, energy density, and power were applied. Recent evidence has suggested that AMSCs exposed to PBMT at 5 J/cm^2 caused pronounced cell proliferation and secretion [41, 46, 47]. Therefore, we speculate that PBMT could enhance AMSCs' treatment potential for fibrotic scar.

Therefore, in this study, we analyzed the key proteins concerned TGF-β and Notch signaling in vitro, to test the effects of conditioned medium gathered from post-PBMT AMSCs (PBMT-AMSCs-CM) on the fibrotic phenotypes associated with hypertrophic scar fibroblasts (HSFs) and keloid fibroblasts (KFs). The outcomes demonstrated that PBMT-AMSCs-CM inhibited cell proliferation and downregulation of the profibrotic growth factor and collagen synthesis associated with HSFs and KFs, especially KFs. Based on our current results, we presume that the inhibiting effect is related to downregulating TGF-β1 and Notch-1 expression.

Materials and methods

Patients and tissue samples

Keloid tissue samples (KD, $n = 14$), hypertrophic scar tissues (HS, $n = 7$), normal skin tissues(NS, $n = 5$), and established fibroblast cell cultures (passage0 to passage4) from the same samples were used in this study. Keloid samples were obtained from individuals who were all consented prior to the surgical procedure, and so were normal skin samples and fat tissue samples from plastic and reconstructive surgery (Supplementary Tab. 1). All the tissues were collected in formalin, Dulbecco's modified Eagle's medium (DMEM, Hyclone, USA), and primary fibroblasts were established as described previously [48].

Isolation and culture of cells

Primary passages of cells from the samples described before were established respectively. After removing subcutaneous tissue, samples were sectioned into small pieces in aseptic culture dish. Then they were digested by collagenase type I (Sigma, USA) in Dulbecco's modified Eagle's medium (DMEM, Hyclone, UT, USA) for an hour prior to centrifugation. After that, fibroblasts could be collected, then seeded to culture dishes, and allowed to adhere and proliferate in a humidified incubator with 5% CO_2 at 37 °C (Thermo Scientific, USA). DMEM was supplemented with 10% fetal bovine serum (FBS, Hyclone, UT, USA) and antibiotics (100 U/ml penicillin and 100 μg/ml streptomycin, Gibco, USA). Each cell population was maintained until confluence, and then trypsinized for seeding. After three or four passages, fibroblasts were used for experiments. Human adipose tissue was obtained from liposuction procedures. Briefly, the lipoaspirate was digested with 0.075% collagenase type I (Sigma, USA) under gentle agitation at 37 °C for 60 min, then centrifuged at 1000 rpm for 10 min to obtain the stromal cell fraction. The pellet was suspended with mesenchymal stem cell medium (Sciencell, USA), then seeded to culture dishes and allowed to adhere and proliferate in a humidified incubator with 5% CO_2 at 37 °C (Thermo Scientific, USA). At 80–90% confluency, AMSCs were trypsinized for seeding. Only passage 3 hAMSCs were used for this study.

Preparation of conditioned medium

The hAMSCs at passage 3 were grown to 80% confluence in DMEM supplemented with 10%FBS, and then incubated with DMEM (without FBS) for 12, 24, and 48 h to collected 12-h-conditioned medium (12 h-CM), 24-h-conditioned medium (24 h-CM), and 48-h-conditioned medium (48 h-CM) separately as positive controls. The 12 h PBMT-AMSCs-CM (12 h-PBMT-CM), 24 h PBMT-AMSCs-CM (24 h-PBMT-CM), and 48 h LLLT-AMSCs-CM (48 h-PBMT-CM) was collected as previously described but with laser irradiation (HairMax LaserComb®, Lexington International, LLC, Boca Raton, Florida) at 12-h intervals. The total surface of the culture dishes was irradiated for 152 s each time; the energy density of the laser was 4 J/cm^2. The dual model device emitted florida 6 laser beams (beam diameter < 5 mm) at a wavelength of 655 nm (± 5%) and 6 laser beams at a wavelength of 635 nm. The conditioned medium was reserved at − 80 °C until required, then thawed overnight (4 °C), and subsequently standardization of the

pH and osmolality before use in the study. The DMEM without AMSCs cultured in incubator for 12, 24, and 48 h separately was used as negative control-conditioned media (Contolr-CM).

Treatment of target fibroblasts with gathered conditioned medium.

Passage 3 or 4 of keloid fibroblasts (KFs), normal skin fibroblasts (NFs), and hypertrophic scar fibroblasts (HSFs) were cultured with prepared conditioned media separately. All dishes were subjected to separate analyses after 24 h, including cell proliferation (Cell Counting Kit 8, CCK-8 assay) and cytotoxicity (LDH) assays, cell cycle behavior (flow cytometry), cell scratch wound-healing assay, collagen I synthesis (hydroxyproline content detection), protein expression (immunofluorescene staining, immunohistochemistry, and Western blotting), and gene expression profiles (real-time PCR).

Cell proliferation (CCK-8), cell apoptosis(MUSE), and cytotoxicity (LDH) assays

Fibroblast cells (KFs, HSFs, and NFs at a density of 2000cells/well) were seeded in 96-well plates with DMEM for 24 h, and then treated with vehicle control (N-CM), and prepared CM separately. In addition, 24 h post-treatment LDH (Dojindo, Japan), CCK-8 (Dojindo, Japan), cell apoptosis (MCH100105, Millipore, Germany) assays were performed according to the manufacture's introductions.

Scratch wound-healing assay

Fibroblasts were seeded in 6-well plates at a density of 50,000 cells/well and culture with complete medium until confluent. Washing with 0.01 M PBS for three times to remove the cell debris. And after 24 h of starvation (DMEM), cells were subjected to a straight scratch induced by a 200 μl pipette tip. Then washing with 0.01 M PBS for three times to remove the cell debris, and treated the cells with vehicle or CM described as before. Graphs of cell migrated to the injury area were taken at 0 and 24 h (Olympus BX5, Japan).

Hydroxyproline content detection

The in-cell hydroxyproline content was detected using a hydroxyproline alkali hydrolysis kit (Nanjing Jiancheng Bioengineering Institute, Nanjing, China). In brief, 24 h post treatments, culture medium was collected and disposed against manufacture's specifications, test reagents were added to the processed samples, and the vehicles and the standers in order separately. The absorbance of the solution was measured at a wavelength of 550 nm, and the levels of hydroxyproline (μg/ml) were calculated by the given formula in the instructions.

RNA extraction, cDNA synthesis, and real-time PCR

Fibroblasts cultured in 6-well were treated with vehicles and ADSCs-CMs for 24 h. Then total RNA from fibroblasts samples were lysed with TRIzol (Invitrogen), and extracted according to the protocol. And 2 μg total RNA was used for synthesizing complementary DNA (cDNA), which is used for real-time PCR. Real-time PCR was performed in triplicate on an ABI Prism 7300 Real-Time PCR System (Applied Biosystems, California, America) in 50 μL reaction mixtures. The reaction conditions were polymerase activation at 95 °C for 5 min, 40 cycles of denaturation at 95 °C for 15 s, and annealing and extension at 62 °C for 35 s. The relative quantification of gene expression was normalized to the expression of endogenous GAPDH. The primer sequences are described in Supplementary Table 2.

Western blot

Briefly, proteins were extracted from cultured cells at 24 h after the treatment for each group, and quantified using the BCA Protein Assay Kit (Cat No. CW0014, CWBIO, China). Equal amounts of protein were subjected to SDS-PAGE and transferred to polyvinylidene fluoride (PVDF) membranes. The primary antibodies (Supplementary Table 3) used for the Western blot were 1:1000 (Abcam, USA). All experiments were triplicated.

Immunofluorescene staining,

Cells were washed three times for 5 min each in 0.01 M PBS and then were fixed with 4% paraformaldehyde at room temperature for 15 min. After washing three times for 5 min each in 0.01 M PBS, the cells were blocked with 10% goat serum for 30 min and then incubation with the anti-activated Notch-1 antibody (ab8925, Abcam, 1:100, USA), anti-TGF beta 1 antibody (ab27969, Abcam, 1:200, USA), and anti-alpha smooth muscle actin antibody (ab7817, Abcam, 1:100, USA) at 4 °C overnight. This was followed by a 40-min incubation with goat anti-rabbit (IgG Alexa Fluor-488, ab150077, Abcam, 1:200, USA) and goat anti-mouse (IgG Alexa Fluor-647, ab150115, Abcam, 1:200, USA) secondary antibodies. After rinsing with PBS, nuclei were stained by DAPI (Abcam, USA). Then the samples were observed under a fluorescence microscope (Leica, Germany, 400–800 nm).

Immunohistochemistry

KD, HS, and NS tissues were fixed in 10% formalin and dehydrated, and then sectioned for paraffin embedding. For immunostaining, 4 μm paraffin sections were incubated in 3%H_2O_2 diluted by methanol for 10 min, followed by washing three times with 0.01 M PBS, and then boiled in 0.01 M citric acid for 2 min. Sections were blocked with 5% bovine serum albumin (BSA) and then incubated with different primary antibodies at 4 °C overnight. After washing the sections in 0.01 M PBS for three times, sections were incubated with secondary antibody for 40 min at room temperature. Sections were detected by DAB kit (ZSGB-bio Beijing, China).

Statistical analysis of data sets

Statistical comparisons between groups were performed using ANOVA analysis by software (version 6.0c, Graphpad Prism). $P < 0.05$ was considered significant.

Results

Differential expression and localization of TGF-β1, Notch1, and smooth muscle α-actin in tissue samples

Immunohistochemistry of tissue samples shows expression of Notch1, TGF-β1, and smooth muscle α-actin (α-SMA) in dermal cells around small glands and microvessels, mostly confined to the cell cytoplasm. Significantly, we noted high levels of these specific antibodies in KD ($n = 22$) compare to that of HS ($n = 18$). However, in the NS ($n = 7$), these antibodies were barely detected. Taken together, we concluded that Notch1, TGF-β1, and α-SMA were overexpressed in KD and HS, especially KD (Fig. 1).

Hydroxyproline content and profibric genes expression were attenuated by condition-media with or without low level laser irradiation.

Hydroxyproline, as a major component of collagen, content of it could predict amount of scar tissue by reflecting collagen levels. As shown in Fig. 2, the hydroxyproline of KFs (Fig. 2a) and HFs (Fig. 2b) was

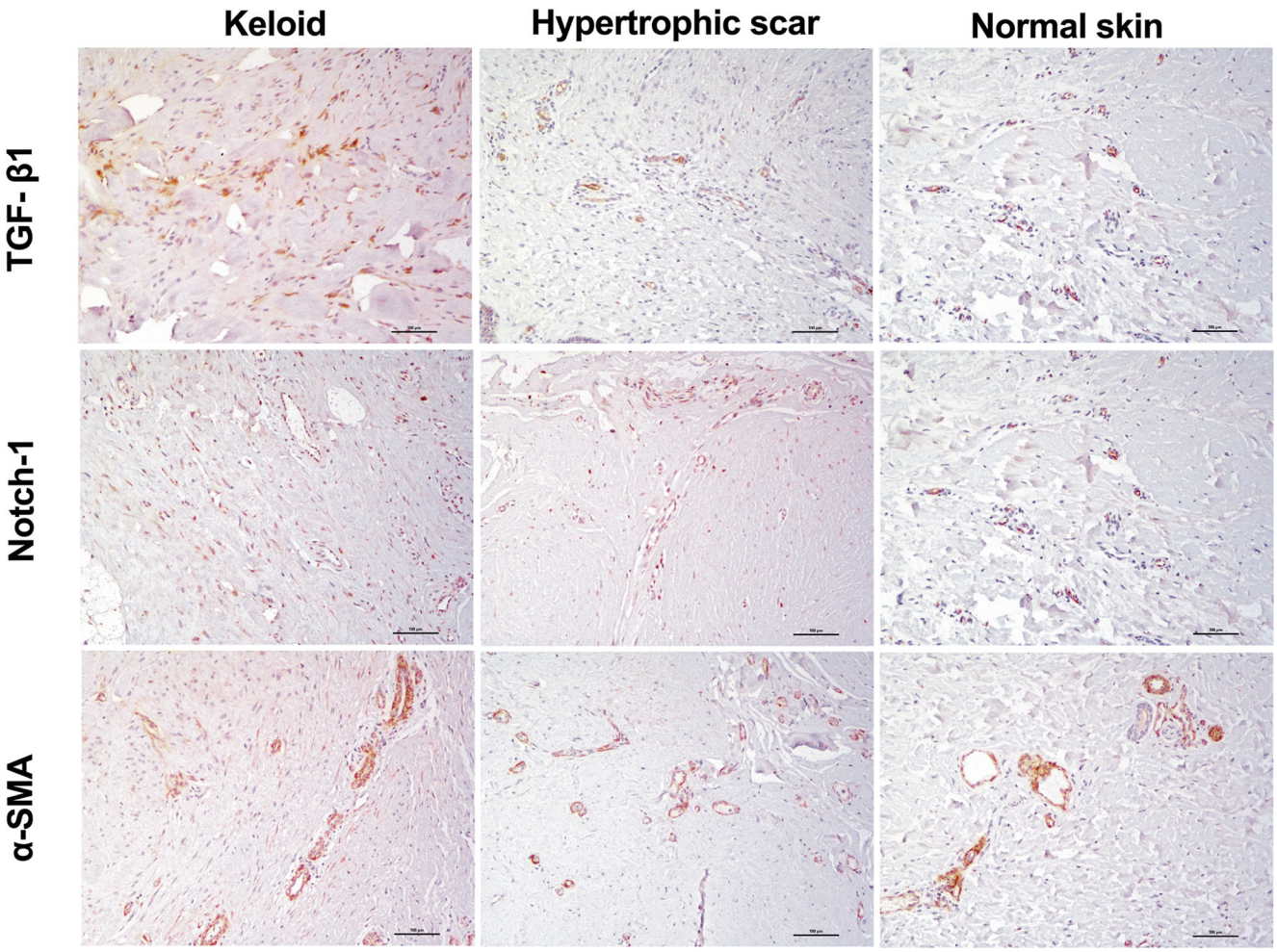

Fig. 1 Immunoreactivity of TGF-β, Notch-1, and α-SMA in keloid, hypertrophic scar, and normal skin tissue. Scale bar = 100 μm

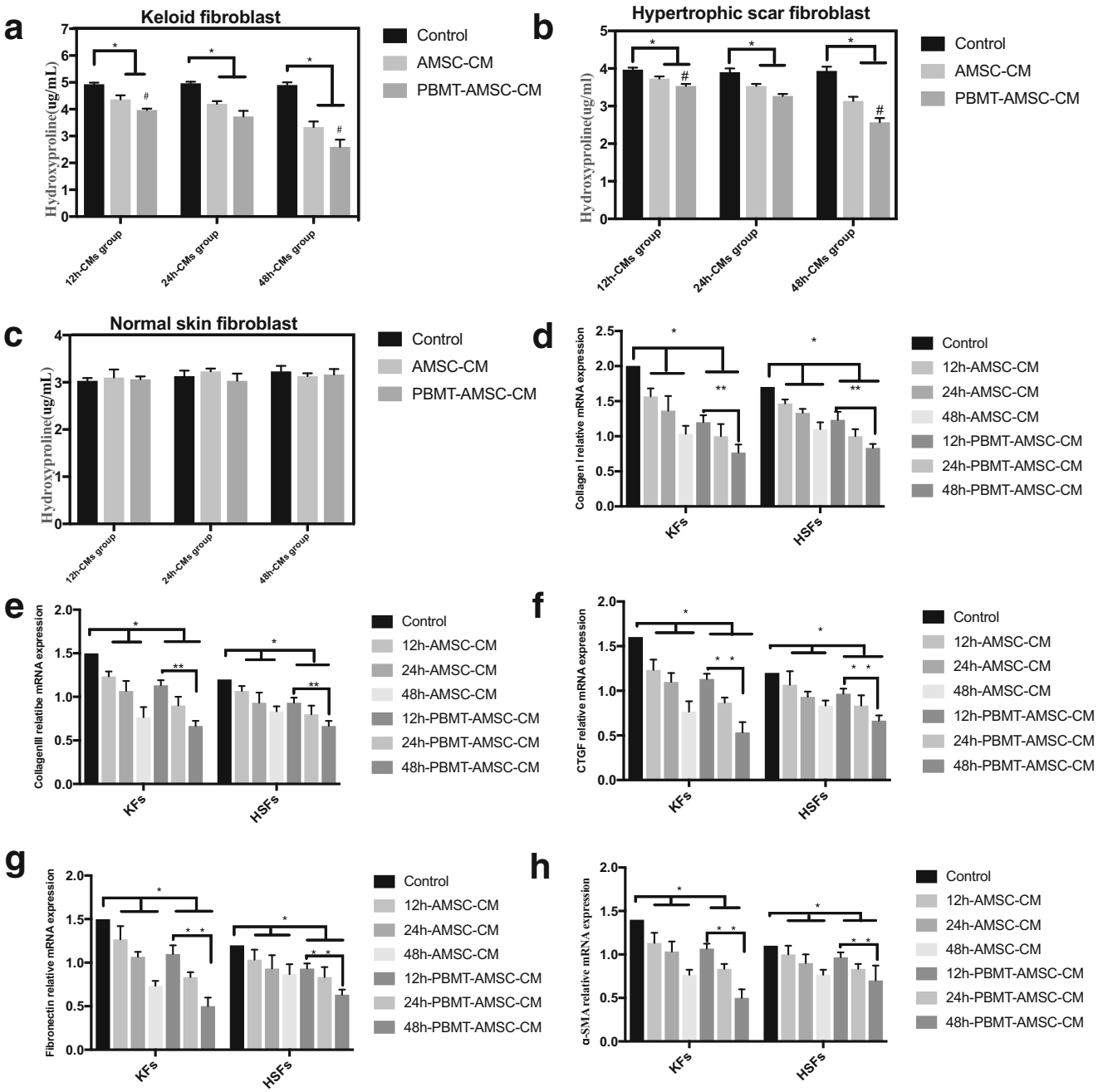

Fig. 2 AMSCs-conditioned medium with or without PBMT-mediated treatment attenuates the profibrotic phenotype of KFs and HSFs. **a**–**c** Cell culture supernatants were collected and tested for hydroxyproline content (mean ± SD, $n = 3$, $*p < 0.05$, compare to the control groups; $\#p < 0.01$, compare the 48h-PBMT-AMSCs-CM groups with the 12h-PBMT-AMSCs-CM). **d**–**h** Quantification of d collagen I, e collagen III, **f** CTGF, **g** fibronectin, and **h** α-SMA gene expression, normalized to GAPDH expression (mean ± SD, $n = 3$, $*p < 0.05$, compare to the control groups; $**p < 0.01$, compare the 48h-PBMT-AMSCs-CM groups with the 12h-PBMT-AMSCs-CM)

significantly decreased after 24 h of incubation with AMSCs condition-media with or without low level laser irradiation in comparison with negative controls, and 48 h-AMSCs-PBMT-CMs treatment groups showed a significant hydroxyproline reduction than that of 12 h-PBMT-AMSCs-CMs. However, effect of CM on NFs is minimal and with no statistical significance (Fig. 2c).

To further determine the association between decrease of hydroxyproline and downregulation of mRNA expression of collagen, RT-PCR analysis was performed for detecting mRNA expression levels of type I and III procollagen. As compared to the vehicle controls, AMSCs-CMs treatment lead to relatively lower expression levels of type I (Fig. 2d) and III (Fig. 2e) procollagen mRNA in KFs and HSFs.

Expression of profibric gene, such as CTGF (Fig. 2f), fibronectin (Fig. 2g), and α-SMA (Fig. 2h), followed the same pattern as procollagen.

Taken together, these results suggest that conditioned media of AMSCs have a function of inhibiting synthesis of ECM in KFs and HSFs, such as collagen, CTGF, fibronectin, and α-SMA; in addition, PBMT mediation could enhance this function, especially in 48 h-PBMT-ADSCs-CMs treatment group.

PBMT-CM is more potent in inhibiting KFs, HSFs proliferation, and migration without cytotoxicity and apoptosis.

After 24 h treatment with CMs, we test the cell proliferation with CCK-8 assay. As shown in Fig. 3a, proliferation rates of KFs and HSFs decreased significantly when incubated in PBMT-AMSCs-CM and AMSCs-CM as compared with negative controlled medium-treated fibroblasts; however, no visible difference was detected when NFs incubated with collected conditioned media. And specifically, 48 h post treatment, inhibited proliferation rate of KFs and HSFs reach a maximum, and then go down till 96 h; this may attribute to cell contact inhibition mechanism. We then measured the effect of described CMs on migration of KFs and HSFs. As results shown in Fig. 3b–d, AMSCs-CM decreased mobility of KFs and HSFs compared with control groups, especially the 48 h-PBMT-ADSCs-CMs. To further investigate the impact of CM described previously, LDH and Annexin V/PI assay was applied; however, no clear difference was detected in cytotoxity and apoptosis among the KFs and HSFs after exposure to AMSC-CM with or without laser irradiation (Fig. 4a, b).

Downregulation of key mRNAs expression in TGF-β1/SMAD3 and Notch-1/JAG-1 signaling in ADSCs-CMs-treatment group was enhanced by LLLT mediation.

Fibroblasts of keloid and hypertrophic scar that undergo fibroproliferative disorder become more proliferative and migratory. And previous findings suggest that Notch1 and TGF-β1 enhanced fibroblast activity in keloid, inducing myfibroblast transition [20, 25]. Our results showed overexpression of Notch1,TGF-β1, and α-SMA in keloid and hypertrophic scar by immunohistochemistry (Fig. 1); overexpression of these factors are also confirmed in fibroblasts cultured from the same sample by immunofluorescence (Fig. 5a). To further explore whether Notch 1 and TGF-β1 play a role in attenuated function of AMSCs-CM on KFs and HSFs, we analyzed gene expression of Notch1 and TGF-β1, of KFs and HSFs post-treatment with CM. As shown in Fig. 5b, c, expression of TGF-β1, Notch-1 were stepwise down-regulated by 12 h, 24 h, 48 h AMSCs-CM compared to control groups in KFs and HSFs after 24-h incubation with collected supernatant, and the inhibition was more pronounced in 48 h PBMT-AMSCs-CMs compared to laser spared 48 h-AMSCs-CM groups separately. In addition, Western blot showed the decrease of TGF-β1and Notch-1

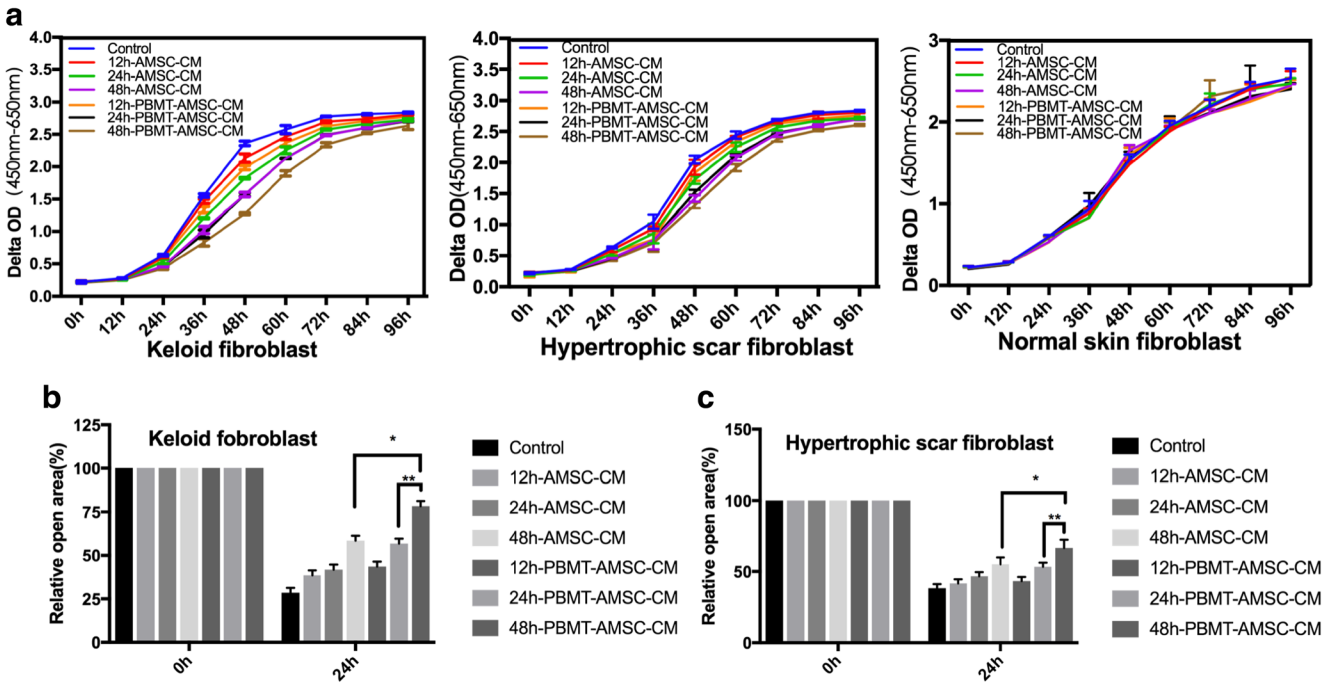

Fig. 3 AMSCs-conditioned medium with or without low level laser mediated inhibits KFs and HFs proliferation and migration. **a** Cell viability was determined by CCK-8 assay every 12 h and compared with the control groups. **b** Cell mobility at six positions (two positions per well) was monitored for each group using a digital imaging microscope and quantified using the Image pro software. **c** Cell mobility was quantified and expressed as relative open areas at the indicated hours with the 0 h as 100% (mean ± SD, $n = 6$, $^{*}p < 0.05$; $^{**}p < 0.01$)

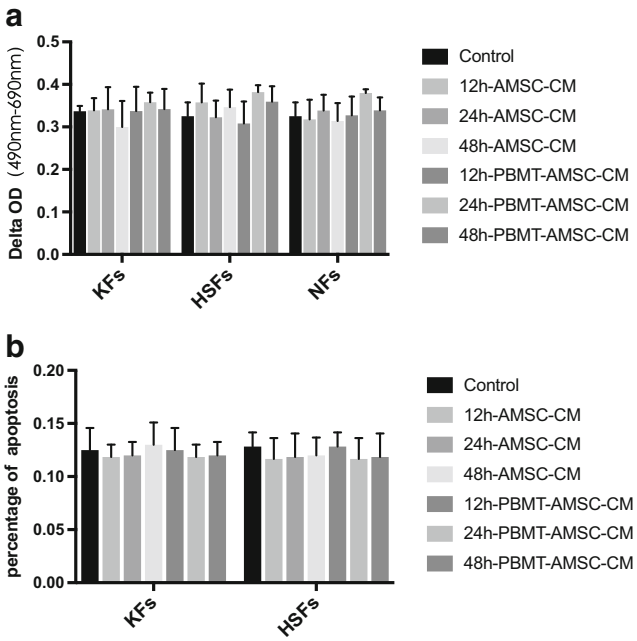

Fig. 4 AMSCs-conditioned medium with or without low level laser mediated does not induce apoptosis and cytotoxicity. **a** LDH assay were used to determine cytotoxicity; the results showed no significant difference. **b** Annexin v pi analysis for the percentage of apoptosis of KFs and HSFs post treatment

at the protein level (Fig. 5d–f). To further detect the TGF-β1and Notch-1 signaling pathway, we test gene expression of their ligands, such as SMAD2, SMAD3 for TGF-β1, and Jagged-1(JAG-1), Jagged-2 (JAG-2), Delta-1for Notch1. Results show downregulation of JAG-1and SMAD3(5G-J), which indicate that paracrine signaling of AMSC may work through Notch1/JAG-1 and TGF-β1/SMAD3 pathway in the context of KFs and HSFs, especially KFs, and the 48 h PBMT-mediated conditioned medium works better than laser free group. Taken together, our results indicate that PBMT-mediated could enhance potential of AMSCs conditioned medium on inhibiting KFs and HSFs proliferation, and this function may act through downregulating expression of key factors included in Notch1/JAG-1 and TGF-β1/SMAD3 signaling pathway.

Discussion

There is growing evidence suggesting that scar remodeling, skin regeneration, and tissue reconstruction have been benefited for paracrine function of AMSCs [49]. Currently, reports indicate that PBMT could increase their therapeutic potential [42, 45, 50].

Therefore, we developed an in vitro research to inquiry whether PBMT enhances the anti-fibrotic capacity of AMSCs on KFs and HSFs, and diving into underlying mechanisms by which AMSCs to take effect.

Results obtained from our experiments showed that cell culture supernatant of post-PBMT AMSCs has much more potential as a fibrotic treatment of KFs and HSFs, and acting by inhibition of the proliferation, migration, and profibrotic genes synthesis via downregulating TGF-β1 and Notch-1 expression.

Keloid scars and hypertrophic scars have been considered to follow fibroproliferative disorder post cutaneous injury, presented with excessive proliferation of fibroblasts and extracellular matrix deposition. Cellular signals released by neighboring cells, such as neutrophils, macrophages, and myofibroblasts, regulates a wide array of biological activities in KFs and HSFs at different wound healing phases [9]. As shown in previous studies, inflammatory-immunological reactions not only play a critical role in the earliest phases but also involved in subsequent profibrotic processes [51]. Dysregulation of three TGF-β isoforms secreted by inflamed immune cells around the wound area prominently mediating formation of keloid and hypertrophic scar, especially TGF-β1, which has been considered as a driving force [52]. Recent evidence shows that immune cells related Notch1 presenting a critical role in the activation of keloid fibroblast, and in addition, Notch-1 and TGF-β-1 signaling can cooperatively regulate variety of cell bioactivities at multiple levels [22–24, 53, 54]. Despite the well-documented cooperation between Notch 1and TGF-β1, whether they act in the context of ADSCs-mediated inhibition of KD and HS has not been studied. By screening of 14 keloid samples, 7 hypertrophic scar tissues, and 5normal skin sections, it showed prominent

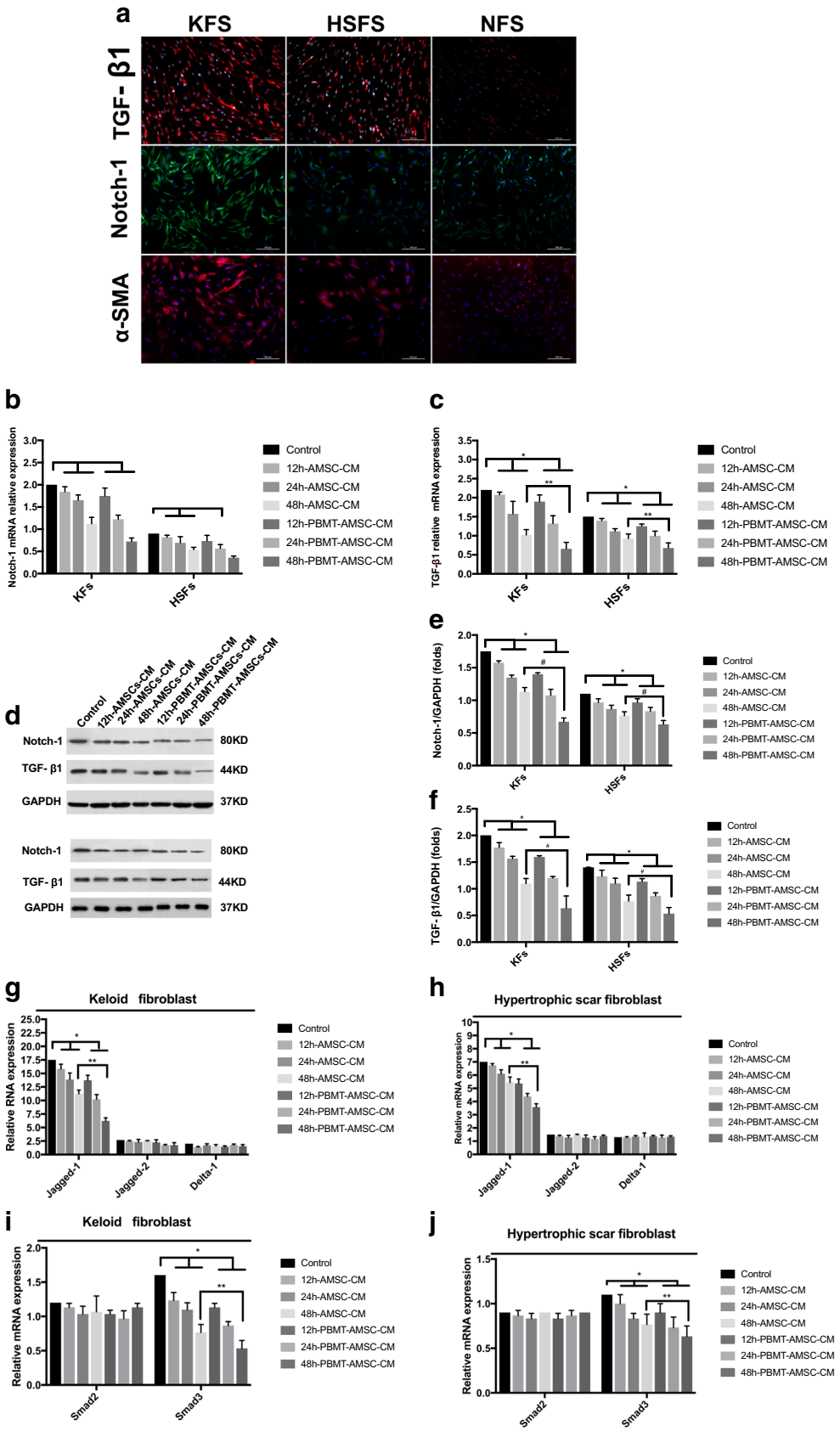
a
KFS
HSFS
NFS
TGF- β1
Notch-1
α-SMA
b
Notch-1 mRNA relative expression
KFs
HSFs
Control
12h-AMSC-CM
24h-AMSC-CM
48h-AMSC-CM
12h-PBMT-AMSC-CM
24h-PBMT-AMSC-CM
48h-PBMT-AMSC-CM
c
TGF-β1 relative mRNA expression
d
Control
12h-AMSCs-CM
24h-AMSCs-CM
48h-AMSCs-CM
12h-PBMT-AMSCs-CM
24h-PBMT-AMSCs-CM
48h-PBMT-AMSCs-CM
Notch-1
TGF- β1
GAPDH
80KD
44KD
37KD
e
Notch-1/GAPDH (folds)
f
TGF- β1/GAPDH (folds)
g
Keloid fibroblast
Relative RNA expression
Jagged-1
Jagged-2
Delta-1
h
Hypertrophic scar fibroblast
Relative mRNA expression
i
Keloid fibroblast
Relative mRNA expression
Smad2
Smad3
j
Hypertrophic scar fibroblast
Relative mRNA expression

◀ **Fig. 5** AMSCs-conditioned medium with or without PBMT downregulated Notch1, TGF-β1 in KFs and HSFs **a** Immunofluorescence staining of TGF-β1, Notch-1 and α-SMA (Scale bar = 200 μm). **b**, **c** mRNA expression variation of TGF-β1 and Notch-1, **d**–**f** western-blot to detected protein change of TGF-β1 and Notch-1 post treatment, and key ligands of TGF-β1 and Notch-1 signaling pathway at mRNA level, **g**–**j** mRNA expression variation of Jagged-1, Jagged-2, Delta-1, Smad2, Smad3 (mean ± SD, $n = 3$, $^{*}p < 0.05$, $\#p < 0.01$, $^{**}p < 0.01$)

overexpression of Notch 1and TGF-β1 in KD when compared to HS, and subsequently confirmed at mRNA and protein levels. However, expression of Notch1 and TGF-β1 in NS was minimal. Then further researches were taken; we isolated and cultured fibroblasts from the samples above, and treated with AMSCs-CM with or without laser-mediated. Our results show that AMSCs-CM has a suppressive effect on the proliferation and migration of KFs and HSFs. In addition, AMSCs-CM can also attenuate synthesis of collagen, and mRNA expression of CTGF, fibronectin, and α-SMA.

CTGF is involved in migration and proliferation of fibroblasts, and synthesis of ECM during wound healing, and it assists TGF-β1 in fibrogenesis and subsequently sustain fibrosis. Collagen I and fibronectin are major identified components of ECM, and can also be regulated by canonical TGF-β1/SMAD3 pathway. Not to mention the myofibroblast differentiation driven by TGF-β1, which classically express α-SMA, and gain the ability of increased migration and proliferation. These results suggest that AMSCs-CM gathered previously do inhibit essential procedure of scaring. More than that, as shown in our results, LLLT can enhance this anti-fibrotic potential of AMSCs on KFs and HSFs. We assume that this beneficial effect may act through downregulation of TGF-β signaling. And lately, Notch1 have been shown to be a crucial role for fibrogenesis and activation of dermal fibroblasts as TGF-β1. Thus, by further understanding of the possible role of Notch 1and TGF-β1 at the functional level in KD and HS, we observed that KFs and HSFs shows an overexpression of Notch1, JAG-1, TGF-β1, SMAD3 at transcriptional level as compared to NFs. These overexpressed profibrotic genes are concerned with Notch1/JAG-1 and TGF-β1/SMAD3 signaling pathway, which play a critical role in fibrosis pathogenesis. Thus, paracrine signaling of AMSCs may make its contribution to moderating fibrotic phenotype of KFs and HSFs by inhibiting Notch1/JAG-1 and TGF-β1/SMAD3 signaling pathways, especially in KFs. Moreover, LLLT enhanced AMSCs paracrine function through an exposure-time-dependent manner as detailed previously.

In summary, our study demonstrates that in vitro LLLT applied to AMSCs boosts its secretion of paracrine factors, thereby enhancing AMSCs potential as a treatment for KFs and HSFs via downregulation of Notch1 and TGF-β1. However, there are limitations of this study that needs further amelioration. Following research is finding out key factors of AMSCs that contributed, and then blocking Notch 1and TGF-β1 pathway separately to detect their relationship in context of KD and HS.

Compliance with ethical standards

Ethical approval and patient consent received.

Conflict of interest The authors declare that they have no conflict of interest.

References

1. Har-Shai Y et al (2006) Intralesional cryosurgery enhances the involution of recalcitrant auricular keloids: a new clinical approach supported by experimental studies. Wound Repair Regen 14(1):18–27
2. Hosnuter M et al (2007) The effects of onion extract on hypertrophic and keloid scars. J Wound Care 16(6):251–254
3. Jacob SE et al (2003) Topical application of imiquimod 5% cream to keloids alters expression genes associated with apoptosis. Br J Dermatol 149(Suppl 66):62–65
4. Gold MH et al (2014) Updated international clinical recommendations on scar management: part 2—algorithms for scar prevention and treatment. Dermatol Surg 40(8):825–831
5. Allendorff J, Riegel W, Kohler H (1997) Regression of retroperitoneal fibrosis by combination therapy with tamoxifen and steroids. Med Klin (Munich) 92(7):439–443
6. Jones CD et al (2015) The use of chemotherapeutics for the treatment of keloid scars. Dermatol Reports 7(2):5880
7. Nakashima M et al (2010) A genome-wide association study identifies four susceptibility loci for keloid in the Japanese population. Nat Genet 42(9):768
8. Ogawa R et al (2014) Associations between keloid severity and single-nucleotide polymorphisms: importance of rs8032158 as a biomarker of keloid severity. J Investig Dermatol 134(7): 2041–2043
9. Berman B, Maderal A, Raphael B (2017) Keloids and hypertrophic scars: pathophysiology, classification, and treatment. Dermatol Surg 43(Suppl 1):S3–s18
10. Bagabir R et al (2012) Site-specific immunophenotyping of keloid disease demonstrates immune upregulation and the presence of lymphoid aggregates. Br J Dermatol 167(5):1053–1066
11. Arima J et al (2015) Hypertension: a systemic key to understanding local keloid severity. Wound Repair Regen 23(2):213–221
12. Huang C, Ogawa R (2014) The link between hypertension and pathological scarring: does hypertension cause or promote keloid and hypertrophic scar pathogenesis? Wound Repair Regen 22(4): 462–466
13. López-Novoa JM, Nieto MA (2009) Inflammation and EMT: an alliance towards organ fibrosis and cancer progression. EMBO Mol Med 1(6–7):303
14. Thiery JP, Sleeman JP (2006) Complex networks orchestrate epithelial-mesenchymal transitions. Nat Rev Mol Cell Biol 7(2):131
15. Yan C et al (2010) Epithelial to mesenchymal transition in human skin wound healing is induced by tumor necrosis factor-α through bone morphogenic protein-2. Am J Pathol 176(5):2247–2258
16. Quaggin SE, Kapus A (2011) Scar wars: mapping the fate of epithelial-mesenchymal-myofibroblast transition. Kidney Int 80(1):41–50
17. Wendt MK, Allington TM, Schiemann WP (2009) Mechanisms of the epithelial-mesenchymal transition by TGF-beta. Future Oncol 5(8):1145
18. Zhang J et al (2014) TGF-β-induced epithelial-to-mesenchymal transition proceeds through stepwise activation of multiple feedback loops. Sci Signal 7(345):ra91

19. Hahn JM et al (2016) Partial epithelial-mesenchymal transition in keloid scars: regulation of keloid keratinocyte gene expression by transforming growth factor-β1. Burns Trauma 4(1):30
20. Syed F, Bayat A (2012) Notch signaling pathway in keloid disease: enhanced fibroblast activity in a Jagged-1 peptide-dependent manner in lesional vs. extralesional fibroblasts. Wound Repair Regen 20(5):688–706
21. Ingrid E et al (2013) Notch signaling: targeting cancer stem cells and epithelial-to-mesenchymal transition. Onco Targets Ther 6:1249
22. Matsuno Y et al (2012) Notch signaling mediates TGF-beta1-induced epithelial-mesenchymal transition through the induction of Snai1. Int J Biochem Cell Biol 44(5):776–789
23. Zhou J et al (2016) Notch and TGFbeta form a positive regulatory loop and regulate EMT in epithelial ovarian cancer cells. Cell Signal 28(8):838–849
24. Wang Y et al (2017) Notch signaling mediated by TGF-beta/Smad pathway in concanavalin A-induced liver fibrosis in rats. World J Gastroenterol 23(13):2330–2336
25. Huang C, Ogawa R (2012) Fibroproliferative disorders and their mechanobiology. Connect Tissue Res 53(3):187–196
26. Kalodimou VE (2016) Isolation of mesenchymal stem cells for the treatment of lung fibrosis in an animal model. J Tissue Sci Eng 7: 2(Suppl). https://doi.org/10.4172/2157-7552.C1.024
27. Lee MJ et al (2010) Anti-fibrotic effect of chorionic plate-derived mesenchymal stem cells isolated from human placenta in a rat model of CCl4-injured liver: potential application to the treatment of hepatic diseases. J Cell Biochem 111(6):1453
28. Leung VYL et al (2014) Mesenchymal stem cells reduce intervertebral disc fibrosis and facilitate repair. Stem Cells 32(8): 2164–2177
29. Ojeh N et al (2015) Stem cells in skin regeneration, wound healing, and their clinical applications. Int J Mol Sci 16(10):25476–25501
30. Spiekman M et al (2014) Adipose tissue-derived stromal cells inhibit TGF-β1-induced differentiation of human dermal fibroblasts and keloid scar-derived fibroblasts in a paracrine fashion. Plast Reconstr Surg 134(4):699
31. Uysal CA et al (2014) The effect of bone-marrow-derived stem cells and adipose-derived stem cells on wound contraction and epithelization. Adv Wound Care 3(6):405–413
32. Zhang Q et al (2015) Intralesional injection of adipose-derived stem cells reduces hypertrophic scarring in a rabbit ear model. Stem Cell Res Ther 6(1):145
33. Zonari A et al (2015) Polyhydroxybutyrate-co-hydroxyvalerate structures loaded with adipose stem cells promote skin healing with reduced scarring. Acta Biomater 17:170
34. Anders JJ, Lanzafame RJ, Arany PR (2015) Low-level light/laser therapy versus photobiomodulation therapy. Photomed Laser Surg 33(4):183
35. Gaida K et al (2004) Low level laser therapy—a conservative approach to the burn scar? Burns 30(4):362
36. Huang YY et al (2009) Biphasic dose response in low level light therapy. Dose-Response 7(4):358
37. de Villiers JA, Houreld NN, Abrahamse H (2011) Influence of low intensity laser irradiation on isolated human adipose derived stem cells over 72 hours and their differentiation potential into smooth muscle cells using retinoic acid. Stem Cell Rev 7(4):869–882
38. Galvão BCA et al (2014) Low-level laser irradiation inducesin vitroproliferation of mesenchymal stem cells. Einstein 12(1):75
39. Kushibiki T et al (2015) Low reactive level laser therapy for mesenchymal stromal cells therapies. Stem Cells Int 2015(6): 974864
40. Park IS, Chung PS, Ahn JC (2014) Enhanced angiogenic effect of adipose-derived stromal cell spheroid with low-level light therapy in hind limb ischemia mice. Biomaterials 35(34):9280–9289
41. Mvula B, Moore TJ, Abrahamse H (2010) Effect of low-level laser irradiation and epidermal growth factor on adult human adipose-derived stem cells. Lasers Med Sci 25(1):33–39
42. Shen CC et al (2013) Low-level laser stimulation on adipose-tissue-derived stem cell treatments for focal cerebral ischemia in rats. Evid Based Complement Alternat Med 2013:594906
43. Min KH et al (2015) Effect of low-level laser therapy on human adipose-derived stem cells: in vitro and in vivo studies. Aesthet Plast Surg 39(5):778–782
44. Wang Y et al (2016) Photobiomodulation of human adipose-derived stem cells using 810nm and 980nm lasers operates via different mechanisms of action. Biochim Biophys Acta 1861(2):441
45. Constantin A et al (2017) CO2 laser increases the regenerative capacity of human adipose-derived stem cells by a mechanism involving the redox state and enhanced secretion of pro-angiogenic molecules. Lasers Med Sci 32(1):117–127
46. Mvula B, Abrahamse H (2016) Differentiation potential of adipose-derived stem cells when cocultured with smooth muscle cells, and the role of low-intensity laser irradiation. Photomed Laser Surg 34(11):509–515
47. Mvula B et al (2008) The effect of low level laser irradiation on adult human adipose derived stem cells. Lasers Med Sci 23(3): 277–282
48. Rittié L, Fisher GJ (2005) Isolation and culture of skin fibroblasts. Methods Mol Med 117:83
49. Gaur M, Dobke M, Lunyak VV (2017) Mesenchymal stem cells from adipose tissue in clinical applications for dermatological indications and skin aging. Int J Mol Sci 18(1):208. https://doi.org/10.3390/ijms18010208
50. Xu X et al (2014) Adipose-derived stem cells cooperate with fractional carbon dioxide laser in antagonizing photoaging: a potential role of Wnt and beta-catenin signaling. Cell Biosci 4:24
51. Wick G et al (2013) The immunology of fibrosis. Annu Rev Immunol 31:107–135
52. MacDonald EM, Cohn RD (2012) TGFbeta signaling: its role in fibrosis formation and myopathies. Curr Opin Rheumatol 24(6): 628–634
53. Aoyagi-Ikeda K et al (2011) Notch induces myofibroblast differentiation of alveolar epithelial cells via transforming growth factor-{beta}-Smad3 pathway. Am J Respir Cell Mol Biol 45(1):136–144
54. Luo K (2017) Signaling cross talk between TGF-beta/Smad and other signaling pathways. Cold Spring Harb Perspect Biol 9(1). https://doi.org/10.1101/cshperspect.a022137